Interacting stochastic oscillators

Jiajun Zhang,[1] Zhanjiang Yuan,[1] Junwei Wang,[1] and Tianshou Zhou[2,1,*]

[1]*School of Mathematics and Computational Science, Sun Yat-Sen University, Guangzhou 510275, China*

[2]*State Key Laboratory of Biocontrol and Guangzhou Center for Bioinformatics, School of Life Science, Sun Yat-Sen University, Guangzhou 510275, China*

(Received 28 September 2007; revised manuscript received 6 December 2007; published 5 February 2008)

Stochastic coherence (SC) and self-induced stochastic resonance (SISR) are two distinct mechanisms of noise-induced coherent motion. For interacting SC and SISR oscillators, we find that whether or not phase synchronization is achieved depends sensitively on the coupling strength and noise intensities. Specifically, in the case of weak coupling, individual oscillators are insensitive to each other, whereas in the case of strong coupling, one fixed oscillator with optimal coherence can be entrained to the other, adjustable oscillator (i.e., its noise intensity is tunable), achieving phase-locking synchronization, as long as the tunable noise intensity is not beyond a threshold; such synchronization is lost otherwise. For an array lattice of SISR oscillators, except for coupling-enhanced coherence similar to that found in the case of coupled SC oscillators, there is an optimal network topology degree (i.e., number of coupled nodes), such that coherence and synchronization are optimally achieved, implying that the system-size resonance found in an ensemble of noise-driven bistable systems can occur in coupled SISR oscillators.

DOI: 10.1103/PhysRevE.77.021101 PACS number(s): 05.40.Ca, 05.45.Xt

I. INTRODUCTION

Rhythm generation is a long-standing problem in science, particularly in biological and cognitive science contexts [1,2]. A paradigm of this kind of self-sustained oscillating behavior in nonlinear systems is offered by the limit cycle. Even in the absence of a limit cycle, however, internal rhythms can be generated in nonlinear systems due to the effect of noise. This phenomenon is the so-called noise-induced coherent motion, which has become an active topic mostly because of its enormous relevance in numerous applications in such fields as engineering, physics, biology, and medicine [3]. There are two distinct mechanisms that can generate such a motion: One is stochastic resonance (SR), where noise at a proper intensity can optimize the response of a nonlinear system to a subthreshold periodic signal [4], or where a dynamical system near but before a Hopf or saddle-node bifurcation threshold is driven by small noise without a periodic signal, then the original potential limit cycle is capable of being excited, and the excited limit cycle emerges right after the bifurcation (the phenomenon in the latter case is traditionally called coherent resonance) [5]. Such features of SR oscillators are well known and often called coherence resonance, autonomous stochastic resonance, or stochastic coherence [6–10]. However, for clarity we prefer and will use the term stochastic coherence (SC) instead of coherence resonance because the former emphasizes the stochastic inducement of periodicity (coherence) in which there may be no explicit "resonance" effect [10–12]. The other mechanism is self-induced stochastic resonance (SISR) described recently in [13–15], which is effective within a larger distance from the bifurcation point.

Lee DeVille *et al.* [14] analyzed what controls the degree of coherence in SC and SISR of the FitzHugh-Nagumo system, and classified their very different properties. They found that SC arises only at the onset of bifurcation and is rather insensitive to variations in noise intensity. In contrast, SISR may arise away from bifurcation, and the property of noise-induced coherent motion is controlled by the noise intensity. A question naturally arises: How do these oscillators behave when they interact (e.g., in the case of interacting SC and SISR oscillators, interacting SC oscillators, or an array lattice of coupled SISR oscillators)?

Coupled SC oscillators have demonstrated some interesting phenomena, e.g., noise-enhanced phase synchronization [16], noise-induced spatiotemporal pattern formation [15,17,18], noise-enhanced wave propagation [19,20], array-enhanced stochastic resonance [21–23], and array-enhanced coherence resonance [24–27]. Another interesting phenomenon is the system-size resonance found in an ensemble of noise-driven bistable systems [28]. These phenomena indicate that interacting SC oscillators have rich dynamical behaviors. Accordingly, we can expect that interacting SISR oscillators or interacting SC and SISR oscillators might have properties similar to but also different from those found in interacting SC oscillators.

The purpose of this paper is to describe the effect of interaction between SC and SISR oscillators, and across populations of SISR oscillators, and, in particular, to describe the mechanism and properties of noise-induced and array-enhanced coherent resonance in these kinds of interacting stochastic oscillators. We will characterize the related coherence by the signal-to-noise ratio (S) and the timing precision of information processing by the mean firing rate (M). By numerical simulation, we find that for interacting SC and SISR oscillators S and M of individual oscillators basically remain independent in the case of weak coupling, whereas one fixed oscillator with optimal coherence can be entrained to the other, adjustable oscillator (i.e., its noise intensity is changeable) in the case of strong coupling, and the two oscillators possess different S and M when the noise intensity

*mcszhtsh@mail.sysu.edu.cn

 ©2008 The American Physical Society

of the adjustable oscillator goes beyond a threshold. For an array lattice of SISR oscillators, except for coupling-enhanced coherence similar to that found in the case of coupled SC oscillators, there is an optimal network topology degree (i.e., number of coupled nodes), such that coherence and synchronization are optimally achieved, implying that system-size resonance, an interesting stochastic synchrony found first in an ensemble of noise-driven bistable systems, can occur in interacting SISR oscillators.

II. CHARACTERISTICS OF COHERENCE AND PERIOD IN SC AND SISR OSCILLATORS

As is well known, the FitzHugh-Nagumo (FHN) system is a simple but representative model of excitable neurons [29]. We will study the following version of the FHN model perturbed by noise:

$$\epsilon\dot{x} = x - x^3/3 - y + \sqrt{\epsilon}\xi_1(t), \tag{1}$$

$$\dot{y} = x + a + \xi_2(t), \tag{2}$$

where x and y represent the fast activation variable and slow recovery variable, respectively; ϵ (we fix $\epsilon=0.01$ throughout this paper) and a are a time scale and a bifurcation parameter, respectively; and $\xi_i(t)$ $(i=1,2)$ are assumed to be independent Gaussian noise sources with zero mean and correlation $\langle \xi_i(t)\xi_j(t')\rangle = D_i\delta_{ij}\delta(t-t')$, $i=1,2$, in which D_i represents the intensity of noise $\xi_i(t)$. In the absence of noise, for $|a|>1$ the system has only a stable fixed point corresponding to the quiescent state of this system, while for $|a|<1$ there exists a globally stable limit cycle. When an appropriate random perturbation ($D_1>0$ or $D_2>0$) acts on the system, the trajectories of the variables $x(t)$ and $y(t)$ in the so-called excitable regime characterized by $|a|>1$ eventually exit the attraction basin of the stable fixed point, and return to it after a large excursion (forming a pulse) in phase space. The regularity of the pulses demonstrates coherent motion in a noisy environment. For an appropriately chosen $a>1$, we can have SC and SISR oscillators which correspond to $D_1=0$, $D_2>0$ and $D_2=0$, $D_1>0$, respectively. For the SC and SISR oscillators, some features about coherence were described in Ref. [14], but here we describe them in different ways and obtain some additional results.

To measure the temporal coherence of noise-induced motion, we introduce an index, denoted by S and defined as

$$S = \frac{\langle T_k\rangle_t}{\sqrt{\mathrm{var}(T_k)}}, \tag{3}$$

where $T_k=\tau_{k+1}-\tau_k$ (here τ_k is the time until the kth firing of the noise-induced oscillator) stands for the distribution of pulse duration, and $\langle\cdots\rangle_t$ denotes an average over time. This index describes the ratio between the average of interspike interval and its standard deviation, and is actually a kind of signal-to-noise ratio in the sense of periodic signals with repetitive firings at a fixed interval. Biologically, this quantity is of importance because it relates to the timing precision of information processing in the neural system [30]. In addition, we introduce the mean firing rate $M=1/\langle T_k\rangle_t$ for a sequence of spikes $\{\tau_k\}$ (i.e., the inverse of the mean interspike interval), which describes the degree to which the neural system encodes information. We are mainly interested in the effect of noise intensities D_i and the parameter a on S and M. All involved stochastic equations throughout this paper are numerically solved using the Heun algorithm with step size $\Delta=10^{-3}$ [31].

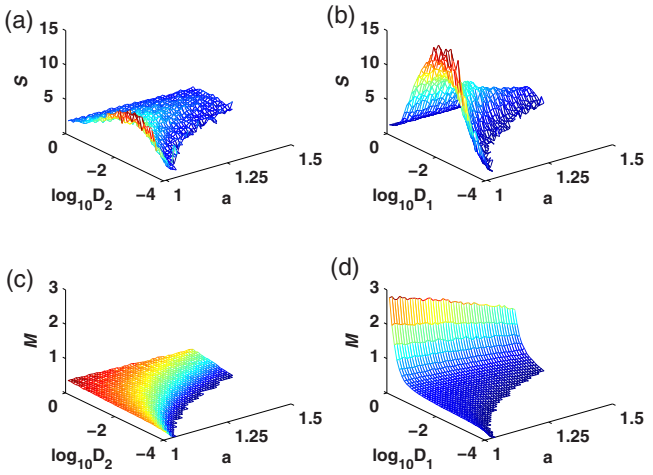

FIG. 1. (Color online) Dependence of S and M on both noise intensity $\log_{10}(D_1)$ or $\log_{10}(D_2)$ and parameter a: (a),(c) $D_1=0$ corresponds to the SC oscillator; (b),(d) $D_2=0$ corresponds to the SISR oscillator.

Figures 1(a) and 1(b) show the dependence of S on both noise intensity and the parameter a, where Fig. 1(a) corresponds to the SC oscillator ($D_1=0$) and Fig. 1(b) to the SISR oscillator ($D_2=0$). A similar feature that is apparent in the cases of SC and SISR oscillators is in stochastic coherence, e.g., for some a near but larger than 1, there is an optimal noise such that S has a maximum in both cases. However, there is a significant difference between the two cases, e.g., for the same value of a, S of SISR is about three times that of SC, indicating that the degree of coherent motion in SISR is dramatically higher than that in SC. Although S decreases monotonically with increase of a in both cases (implying that the coherence is reduced when the bifurcation parameter a departs from the threshold of bifurcation), it is always higher in SISR than in SC for the same pair of parameter values in the parameter region (D_i,a). In particular, S with $a=1.50$ in SISR is roughly equivalent to S with $a=1.01$ in SC. Another outstanding difference appears in that the coherence in SC arises only on the onset of bifurcation, whereas the coherence in SISR may arise far from the bifurcation point and persist even in a broad parameter region of a (according to Ref. [14], a can be up to $\sqrt{3}$).

Figures 1(c) and 1(d) show the dependence of the mean firing rate M on both noise intensity $D_{1,2}$ and the parameter a, respectively. For a given a, this dependence also shows a significant difference in the cases of SC and SISR. Specifically, in the case of SC, M increases as D_2 increases in the low-level noise region, but takes a stable value when D_2 is beyond a threshold, indicating that the mean firing rate is rather insensitive to noise intensity. In contrast, M in the case of SISR is always a monotonically increasing function of D_1,

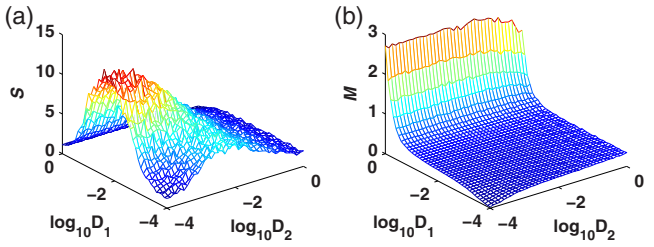

FIG. 2. (Color online) Signal-to-noise ratio S and mean firing rate M in the competitive situation of combined SC and SISR oscillators: (a) S as a function of both $\log_{10}(D_1)$ and $\log_{10}(D_2)$; (b) M as a function of both $\log_{10}(D_1)$ and $\log_{10}(D_2)$. In (a) and (b), $a=1.05$ and $\epsilon=0.01$.

and even can reach an arbitrary value at a large enough D_1, suggesting that the mean firing rate is susceptible to noise intensity in the case of SISR, and that D_1 can thus be used as a controllable parameter for M from the viewpoint of control theory. In spite of this difference in the mean firing rate between the two situations, there are similar features, e.g., M gradually drops for a fixed D_1 or D_2 in both cases as a increases.

To take a step closer to reality, two noise sources should be simultaneously taken into account in the FHN system, since the fast variable corresponding to the membrane potential is subjected to fluctuations and the recovery variable associated with the refractory property of a neuron is often noisy [32,33]. Figure 2(a) illustrates the coherence with fixed $a=1.05$ in the simultaneous presence of two noise sources, used to mimic the competition of combined SC and SISR oscillators. Three features should be noted. First, there is a pronounced maximum of the signal-to-noise ratio S with respect to D_1 as $D_2 \to 0$ or with respect to D_2 as $D_1 \to 0$. In particular, the system (1) and (2) exhibits the characteristics of SC in the case that $D_1 \to 0$ vanishes in the limit, and the characteristics of SISR in the case that $D_2 \to 0$ vanishes in the limit. In other words, SC dominates in the former case whereas SISR dominates in the latter case. Second, if S is considered as a function of D_1 while D_2 is kept at some fixed value, its maximum value at a certain D_1 value is insensitive to slow variable fluctuation for some $D_2 < 10^{-3.0}$. However, it drops rapidly as D_2 increases but keeps $D_2 > 10^{-3.0}$, indicating that the slow variable fluctuation may violate coherence. Finally, we consider S as a function of D_2 for two different ranges of values of D_1. For $D_1 < 10^{-3.0}$, S shows one maximum as D_2 is varied, indicating that the SC mechanism dominates the dynamics, whereas for $D_1 > 10^{-3.0}$, it decreases monotonically as S increases, implying that the noise in the membrane potential can enhance the coherence of the whole system.

Figure 2(b) plots the mean firing rate M as a function of both D_1 and D_2. For low-level noise, e.g., $D_1 < 10^{-3.0}$ and $D_2 < 10^{-3.0}$, both noise sources cooperatively produce a series of pulses, but the pulse events in a given time interval are rather rare, consequently leading to a small M. In particular, in the interval of small noise intensity D_1, M almost stays constant with respect to D_2. However, the noise from the fluctuation of the membrane potential can drastically affect the mean firing rate, e.g., M quickly increases as D_1 increases at a fixed D_2.

III. INTERACTING SC AND SISR OSCILLATORS

Synchronization phenomena not only can take place in a deterministic system composed of regular oscillators, but also can emerge between interacting stochastic oscillators in a statistical sense. The phase locking of two interacting SC oscillators has been investigated [34–36]. In this section we focus on the question to what extent interacting SC and SISR oscillators adjust their respective phases so as to attain some kind of synchronization, and vice versa. For simplification, based on discussions in the previous section, we consider the following mathematical model:

$$\epsilon \dot{x}_1 = x_1 - x_1^3/3 - y_1 + g(x_2 - x_1), \tag{4}$$

$$\dot{y}_1 = x_1 + a_1 + \xi_1(t), \tag{5}$$

$$\epsilon \dot{x}_2 = x_2 - x_2^3/3 - y_2 + g(x_1 - x_2) + \sqrt{\epsilon}\xi_2(t), \tag{6}$$

$$\dot{y}_2 = x_2 + a_2, \tag{7}$$

where a_i $(i=1,2)$ are the bifurcation parameters of SC and SISR oscillators, respectively; g represents coupling strength; and $\xi_i(t)$ $(i=1,2)$ are independent Gaussian noise sources with zero mean and correlation $\langle \xi_i(t)\xi_j(t')\rangle = D_i\delta_{ij}\delta(t-t')$, $i=1,2$ [where D_i is the intensity of noise $\xi_i(t)$ $(i=1,2)$]. In simulations, we set $a_1=a_2=1.05$ to make comparisons between the noise-induced coherence of two stochastic oscillators. Note that for such fixed parameter values both uncoupled systems have a stable fixed point in the absence of noise.

For the SC or SISR oscillator in the interaction case, as in the previous section, we may introduce the corresponding S and M, which are respectively used to measure the temporal coherence of noise-induced motion and to describe the mean firing rate. In addition, we introduce an instantaneous phase for each individual oscillator,

$$\phi_i(t) = 2\pi \frac{t - \tau_k^i}{\tau_{k+1}^i - \tau_k^i} + 2\pi k, \quad \tau_k^i \le t < \tau_{k+1}^i, \tag{8}$$

where τ_k^i is the time until the kth firing of the ith oscillator ($i=1$ corresponds to a SC oscillator and $i=2$ to a SISR oscillator), which is defined in the simulation as the moment of crossing the threshold $x=1.0$ of $x_i(t)$. Finally, we introduce an ordering parameter $R=\langle \sin^2[(\phi_1(t)-\phi_2(t))/2]\rangle_t$ (here $\langle\cdots\rangle_t$ denotes the time average) to measure the phase synchronization effect between SC and SISR oscillators (such a definition for the order parameter was adopted in Refs. [24,37]).

In order to investigate the interaction between SC and SISR oscillators, we consider the following two situations separately: (1) a fixed SC oscillator and an adjustable SISR oscillator; (2) a fixed SISR oscillator and an adjustable SC oscillator. Here, a fixed SC or SISR oscillator means that the isolated SC or SISR oscillator (i.e., uncoupled oscillator) is associated with an optimal noise source that induces the "best" coherent motion, and consequently the corresponding

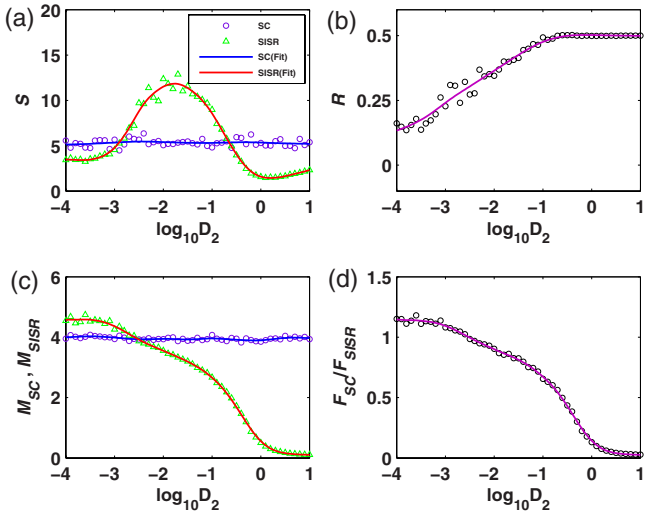

FIG. 3. (Color online) Coherence and synchronization in the case of the fixed SC oscillator and adjustable SISR oscillator with weak coupling $g=10^{-2.0}$. (a) The coherence factor S vs noise intensity D_2. (b) The order parameter R vs D_2. (c) The mean firing period of the SC (M_{SC}) and of the SISR oscillator (M_{SISR}) vs D_2. (d) The ratio of frequencies of SC (F_{SC}) and SISR oscillator (F_{SISR}) vs D_2. In (a),(c) the purple circles and green triangles correspond to SC and SISR, respectively. In (a)–(d), $D_1=10^{-2}$, and the polynomial curves have been fitted to the data to aid the eye.

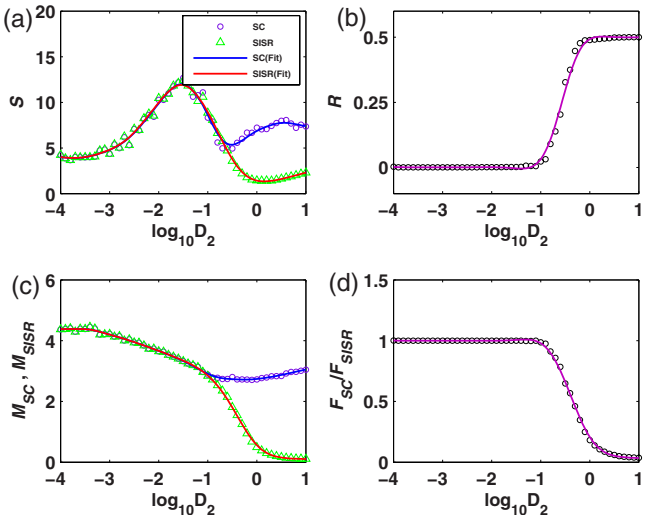

FIG. 4. (Color online) Coherence and synchronization in the case of fixed SC oscillator and adjustable SISR oscillator with strong coupling $g=10^{-1.0}$. (a) The coherence factor S vs noise intensity D_2. (b) The order parameter R vs D_2. (c) The mean firing period of the SC (M_{SC}) and of the SISR oscillator (M_{SISR}) vs D_2. (d) The ratio of frequencies of SC (F_{SC}) and SISR oscillator (F_{SISR}) vs D_2. In (a),(c) the purple circles and green triangles correspond to SC and SISR, respectively. In (a)–(d), $D_1=10^{-2}$, and the polynomial curves have been fitted to the data to aid the eye.

S has the maximal value, whereas for an adjustable oscillator the coherence of the oscillator can be tuned using the noise intensity.

First, we examine the case 1 under two situations of weak and strong coupling (here a "weak coupling" means that the interacting SC and SISR oscillators do not achieve synchronization for this coupling strength; otherwise we have "strong coupling"). For a weak coupling strength, e.g., $g=10^{-2.0}$, the interacting oscillators seem independent of each other. Figure 3(a) shows that the S of the fixed SC oscillator is not affected by the adjustable SISR oscillator. Also, the two oscillators cannot show any collective behavior in the sense of phase synchronization [Fig. 3(b)], frequency locking [Fig. 3(c)], or the ratio of mean firing rates [Fig. 3(d)]. When the coupling strength increases, the two oscillators gradually become sensitive to each other. In particular for strong coupling (e.g., $g=10^{-1.0}$), this sensitivity becomes apparent, as indicated in Fig. 4. In this case, the fixed SC oscillator can be entrained to the adjustable SISR oscillator at a low noise intensity (D_2), so that the two stochastic oscillators achieve phase synchronization and display stochastic frequency locking [Fig. 4(d)], when the noise intensity is below a threshold. However, as D_2 goes beyond the threshold, the frequency locking spreads out because the SISR oscillator fires more frequently than the SC oscillator, so that the difference of average period between the two stochastic oscillators becomes larger, as shown in Fig. 4(c). In other words, the synchronization achieved between the two oscillators can be violated when D_2 is large enough. Moreover, during the gradual disappearance of the achieved synchronization, the S of the SISR oscillator undergoes a continuous decrease and is always below that of the SC oscillator. Within the domain $D_2\in[10^0,10^{1.0}]$, the mean firing period of the SISR oscillator goes down, but the firing becomes more regular and the coherence drops until some critical level of the noise ($D_2=10^{-1.5}$). In particular, as the noise intensity exceeds $10^{-1.0}$, the firing occurs more frequently, but the phase locking and frequency locking start to disappear. More interestingly, the S of the SC oscillator rises again after a minimum value, although the coherence of the SISR oscillator is being reduced all the time. This is mainly because our coupling is introduced in the fast variable. Consequently, the coupling effect can be viewed as the introduction of a noisy perturbation to the SC oscillator, leading to another local maximal S. Therefore, this case can be described as competition between combined SC and SISR oscillators, where the dominant oscillator is the SISR oscillator (see Fig. 2).

Next, we investigate the case 2 in the weak and strong coupling situations. In the case of weak coupling, the results are basically similar to Fig. 3, as shown in Fig. 5, where the interacting oscillators cannot show any phase synchronization except for one case of frequency locking ($D_1\approx 10^{-1.25}$). However, in the case of strong coupling, different phenomena from those demonstrated in Fig. 4 are observed, as shown in Fig. 6. At a low noise intensity D_1, the adjustable SC oscillator does not influence the fixed SISR oscillator, where the former has the same S as the latter. With a further increase of D_1, the coherence of both oscillators is reduced, and at the same time they gradually lose the achieved synchronization. Note that the relative positions of the two curves (for SC and SISR) in Fig. 6 are just opposite to those in Fig. 4 in the nonsynchrony region. This difference can be explained through the effect of two different noise sources.

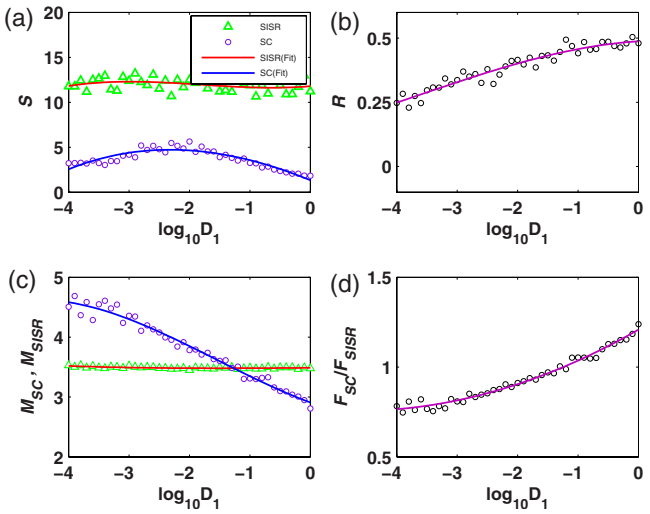

FIG. 5. (Color online) Coherence and synchronization in the case of fixed SISR oscillator and adjustable SC oscillator with a weak coupling strength $g=10^{-2.0}$. (a) The coherence factor S vs noise intensity D_1. (b) The order parameter R vs D_1. (c) The mean firing period of the SC (M_{SC}) and of the SISR oscillator (M_{SISR}) vs D_1; (d) The ratio of frequencies of SC (F_{SC}) and SISR oscillator (F_{SISR}) vs D_1. In (a),(c) the purple circles and green triangles correspond to SC and SISR, respectively. In (a)–(d), $D_2=10^{-2}$, and the polynomial curves have been fitted to the data to aid the eye.

In Fig. 4, the fast variable fluctuation plays a constructive role in the interacting oscillators, e.g., for moderate noise intensities, the fluctuation can enhance the global coherence. In particular, a very strong fast variable noise in one subsystem can produce the maximal S in the other subsystem, but the first subsystem sacrifices its own coherence. In contrast to the fast variable noise, slow variable fluctuation can destroy the global coherent motion. In addition, there is an opposite relation between the mean firing periods (or mean firing rates) in strong coupling for cases 1 and 2 when the noise intensity in the adjustable oscillator is beyond a threshold, which can be shown by comparing Fig. 4(c) and Fig. 6(c) or Fig. 4(d) and Fig. 6(d). Moreover, the period of the adjustable oscillator drops faster than that of the fixed oscillator, implying that the synchronization of interacting SC and SISR oscillators is gradually lost [see Fig. 4(b) and Fig. 6(b)] as the noise intensity in the adjustable oscillator moves beyond a threshold. The differences between cases 1 and 2 can be further shown by comparing Fig. 4(a) and Fig. 6(a). In fact, the curves in Fig. 6(a), unlike those in Fig. 4(a), are monotonically decreasing. (This is possibly because the input stimulus to the SISR oscillator from the SC oscillator cannot induce a good coherent resonance of the SISR oscillator but has a destructive effect on its coherence as the noise intensity in the adjustable SC oscillator goes beyond a threshold.)

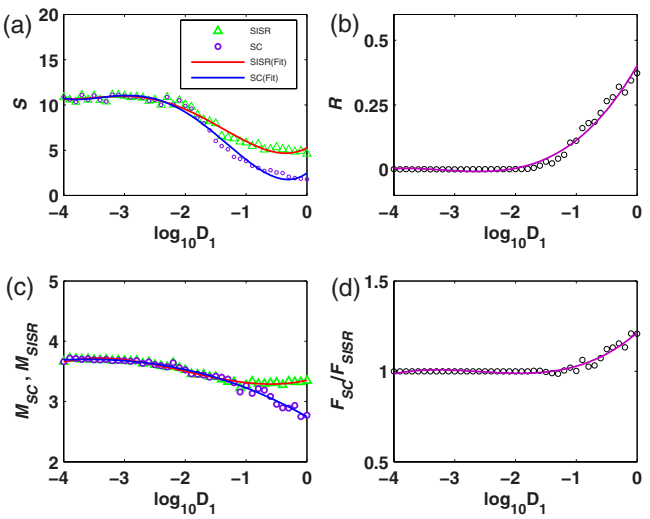

FIG. 6. (Color online) Coherence and synchronization in the case of fixed SISR oscillator and adjustable SC oscillator with a strong coupling strength $g=10^{-1.0}$. (a) The coherence factor S vs noise intensity D_1. (b) The order parameter R vs D_1. (c) The mean firing period of the SC (M_{SC}) and of the SISR oscillator (M_{SISR}) vs D_1; (d) The ratio of frequencies of SC (F_{SC}) and SISR oscillator (F_{SISR}) vs D_1. In (a),(c) the purple circles and green triangles correspond to SC and SISR, respectively. In (a)–(d), $D_2=10^{-2}$, and the polynomial curves have been fitted to the data to aid the eye.

In summary, whether or not the interacting SC and SISR oscillators achieve phase synchronization sensitively depends on both the coupling strength and noise intensities. More precisely, an appropriate coupling strength can make the interacting SC and SISR oscillators achieve phase synchronization if the noise intensity of the adjustable oscillator does not go beyond a threshold, and otherwise the achieved synchronization can also be lost.

IV. ARRAY-ENHANCED SISR

Neurons may be coupled in various forms and receive fluctuating stimuli simultaneously from their neighboring units. Here, we consider a common form of coupling, i.e., a chain of N locally coupled FHN systems, and study the effect of interplay between coupling and noise on coherence. The mathematical equations are

$$\epsilon\dot{x}_i = x_i - x_i^3/3 - y_i + g(x_{i+1} + x_{i-1} - 2x_i) + \sqrt{\epsilon}\xi_{i1}(t), \quad (9)$$

$$\dot{y}_i = x_i + a_i + \xi_{i2}(t), \quad (10)$$

where $\langle \xi_{ik}(t)\xi_{jl}(t')\rangle = D_k\delta_{ij}\delta_{kl}\delta(t-t')$, $i,j=1,\ldots,N$, $k,l=1,2$, D_k represents noise intensity, and g is the coupling strength. We assume the periodic boundary condition $x_0=x_N$, and that a_i is a random variable uniformly distributed in $(a_0-\delta a, a_0+\delta a)$ [24,25,38]. In the following, we set $N=100$, and let $a_0=1.05$, $\delta a=0.05$ (we use the same set of various $\{a_i\}$ from the uniform distribution for all simulations for each run). We try to determine how the coherence and cooperative dynamics of the interacting subsystems depend on coupling strength and noise intensity. For this, we introduce several definitions. (1) We define the instantaneous phase for individual oscillators, as in Eq. (8). (2) The ordering parameter is defined as

$$R = \langle \overline{R_{i,j}} \rangle_t = \lim_{T\to\infty} \int_0^T \left(\frac{1}{M} \sum_{i>j} R_{ij}(t) \right) dt, \quad M = \binom{N}{2}, \quad (11)$$

which is a natural extension of the definition given in the previous section, where $\langle \cdots \rangle_t$ denotes the time average and $\overline{\cdots}$ indicates the ensemble average. Here, the quantity

$$R_{i,j}(t) = \sin^2\left(\frac{\phi_i(t) - \phi_j(t)}{2} \right) \quad (12)$$

is used to measure the phase synchronization effect of neighboring elements [24]. In this way, the numerical simulations display that $R \gtrsim 0.5$ in the unsynchronized regime, whereas $R \approx 0$ in the synchronization regime. (3) We also compute the coherence factor S and mean firing rate M of the chain based on the distribution of pulse intervals of all N oscillators, i.e., $S = \overline{S^i}$, $M = \overline{M^i}$ ($\overline{\cdots}$ stands for the ensemble average over neurons), where

$$S^i = \frac{\langle T_k^i \rangle_t}{\sqrt{\mathrm{var}(T_k^i)}}, \quad (13)$$

$$M^i = 1/\langle T_k^i \rangle_t \quad (14)$$

are the signal-to-noise ratio and mean firing rate of the ith individual neuron ($i = 1, \ldots, N$), respectively.

It should be pointed out that array-enhanced coherence has been investigated in Refs. [24–27], but the setup of the system in our case is different from those papers in the following manner: The fast variable x and the slow variable y are perturbed by the noise either individually or simultaneously, and heterogeneity resulting from the random a_i is considered. However, similar features in the dependence of S and R on g and D are obtained, in contrast to those reported in Refs. [24–27].

The three-dimensional parameter diagrams, as shown in Figs. 7(a) and 7(b), plot the signal-to-noise ratio S as a function of both noise intensity $D_{1,2}$ and coupling strength g. Figure 7(a) with fixed $D_1 = 0.0$ and Fig. 7(b) with fixed $D_2 = 0.0$ correspond, respectively, to coupled SC oscillators and coupled SISR oscillators. These two figures exhibit similar features in shape. For a very weak coupling ($g < 10^{-2.0}$), both S's as a function of noise pass through a maximum and display coherent motion similar to that observed in a single SC or SISR oscillator. With increase of the coupling strength g, the oscillators mutually excite their neighboring elements. Heuristically, coupling favors coherent motion over incoherent motion by increasing S and decreasing R, as shown in Figs. 7(a), 7(b), and 8(a). In the limit of high coupling, the oscillators are rigidly connected but behave as a single oscillator. Consequently, the degree of synchronization (R) approximates to zero, where a pronounced SC scenario is observed again, which looks like a "huge" stochastic oscillator induced by noise. In addition, as the coupling strength gradually increases from a small value, the S peak positions shift from low- to high-level noise. These numerical results indicate that coupling can greatly enhance the self-induced stochastic resonance in a heterogeneous array of coupled FHN

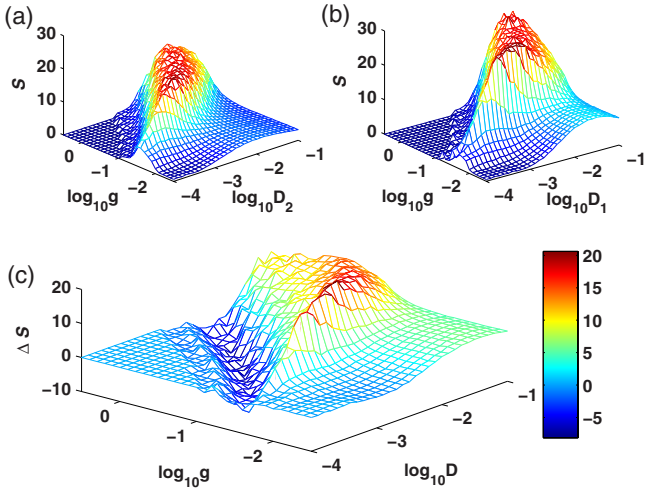

FIG. 7. (Color online) Comparison of the dependence of S on both the noise intensity $\log_{10}(D_{1,2})$ and the coupling strength $\log_{10}(g)$ in the lattice of coupled SC and SISR oscillators. (a) S of the SC, denoted by S_{SC}, where $D_1 = 0.0$. (b) S of the SISR, denoted by S_{SISR}, where $D_2 = 0.0$. (c) The difference $\Delta S = S_{\mathrm{SISR}} - S_{\mathrm{SC}}$, where we set $D_1 = 0$ and $D_2 = D$ when calculating S_{SC} and $D_2 = 0$ and $D_1 = D$ when calculating S_{SISR}.

neurons, similar to array-enhanced coherence resonance. In this case, we prefer instead to use the term array-enhanced self-induced stochastic resonance.

However, there are significant differences between the effects of noise in array-enhanced SC and array-enhanced SISR, as shown in Fig. 7(c). In the following, we analyze these differences.

First, we analyze the occurrence of peaks, valleys, and plateaus in coherence [see Figs. 7(a)–7(c)]. By using S in Fig. 7(b), denoted by S_{SISR}, and S in Fig. 7(a), denoted by S_{SC}, we define $\Delta S = S_{\mathrm{SISR}} - S_{\mathrm{SC}}$, the difference between the coherence factors of the coupled SC oscillators and coupled SISR oscillators [25]. Note the following points. (1) There is a broad peak in the parameter region in Fig. 7(c), indicating that the SISR oscillators in the lattice are more regular than the SC oscillators for most of the parameter values. The gain in S is a consequence of the dominion of the single SISR oscillator and the insensitivity of SISR oscillators to the heterogeneity of parameter a, in comparison with SC oscilla-

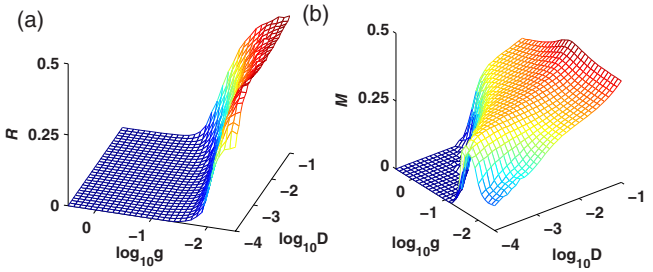

FIG. 8. (Color online) Dependence of order parameter R (a) and mean firing rate M (b) on both the common noise intensity D and the coupling strength g in the lattice of coupled stochastic oscillators, where we assume $D \equiv D_1 = D_2$.

tors. (2) A valley emerges with a particular combination of the coupling strength and noise intensity. In the relevant region, the coupled "SISR oscillators" no longer oscillate because of the strong coupling and relatively small noise in the fast variable, leading to $S=0$. However, for the same parameter values, the coupled SC oscillators still generate moderate coherent motion; thus $S>0$. Therefore, the appearance of a valley can be observed as a result of $\Delta S<0$ [see Fig. 7(c)]. (3) We find one pronounced plateau located in the region of strong coupling strength and low noise intensity, where no firing event is observed in either SC or SISR situation, resulting in the same S value. Note that the difference ΔS is almost equal to or less than zero near the plateau, implying that the coupled SC oscillators have more robust synchronized firings than the coupled SISR oscillators. By combining the results of Fig. 7, we conclude that coupled SISR oscillators would have higher reliability than coupled SC oscillators in information processing.

Second, we investigate the synchronization of stochastic oscillators in the simultaneous presence of two types of noise source. For this, we assume $D \equiv D_1 = D_2$. Coupled stochastic oscillators can display both partial and complete synchronization. The main synchronization features are displayed in Fig. 8(a). For a very weak coupling, the oscillators are essentially independent and behave as if isolated, so that the phase difference between neighboring oscillators follows a uniform random distribution on $(0, 2\pi)$, and consequently $R \approx 0.5$. With increase of the coupling strength, the interacting systems display clustering of synchronization, as shown in the slope of Fig. 8(a). However, they can also demonstrate complete phase synchronization, where all the elements are locked to a common firing rate in the limit of high coupling, as seen in the plateau shown with $R \approx 0$. The above results indicate that interaction between elements in the coupled systems not only causes synchronization of the firing process induced by independent noises, but also greatly improves the coherence of the noise-induced motion.

Finally, we also investigate how the coupling strength and noise intensity affect the mean firing rate, as shown in Fig. 8(b). For a fixed D, M displays a local maximum as g changes, which corresponds to the situation where all oscillators are locked to a relatively large firing frequency. On the other hand, for a given coupling strength g, the M's of SC and SISR seem to increase as D increases.

V. THE EFFECT OF NETWORK TOPOLOGY DEGREE ON COHERENCE

In real networks, one node possibly receives signals from many other nodes. Assume that each node is a stochastic oscillator (SC or SISR oscillator) and receives signals of equal number from its neighboring nodes; this common number is called the network topology degree in this paper. A question naturally arises: How does the network topology degree affect the coherence of the whole interacting system? In this section, we will investigate a one-dimensional array of locally coupled SISR oscillators with a random distribution of the parameter a. The corresponding equations of motion are

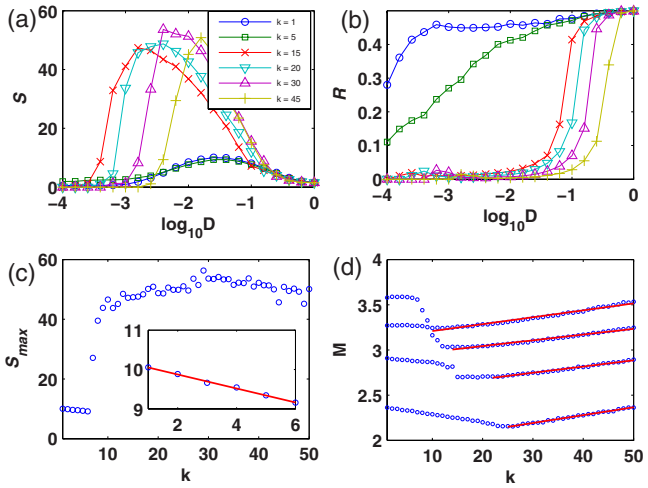

FIG. 9. (Color online) Influence of network topology degree (k) on dynamics of coupled systems with $g=10^{-2.5}$. (a) The coherence factor S vs noise intensity for several values of k. (b) The order parameter R vs noise intensity for the same values of k as in (a) [i.e., the colored curves correspond to those in (a)]. (c) The maximal value of S in the observed noise range vs k. Inset: $S_{\max}$ vs k of 1–6. (d) Mean firing period M vs k for several values of noise intensity, from top to bottom: $D=10^{-2.0}, 10^{-1.6}, 10^{-1.2}, 10^{-0.8}$. The solid lines represent the linear fittings.

$$\epsilon \dot{x}_i = x_i - x_i^3/3 - y_i + g\sum_{j=1}^{k} (x_{i+j} + x_{i-j} - 2x_i) + \sqrt{\epsilon}\xi_i(t), \tag{15}$$

$$\dot{y}_i = x_i + a_i, \tag{16}$$

where $\langle \xi_i(t)\xi_j(t')\rangle = D_i\delta_{ij}\delta(t-t')$, $i=1,\cdots,N$, D_i represents the noise intensity, g is coupling strength, and a_i is the bifurcation parameter of the ith subsystem $[i=1,\ldots,N\ (=100)]$. To mimic the diversity of coupled neurons, we assume that these a_i obey a uniform distribution with mean $a=1.05$ and $\delta a=0.05$. $x_{-i}=x_{N-i}$, $i=1,\ldots,N$, due to the circular property of the network topology, and k is the number of signals that each stochastic oscillator receives from the other units. In this paper we call a coupled system with the coupling form of Eqs. (15) and (16) a density-coupled system. Note that $k=1$ corresponds to nearest-neighboring coupling and $k=(N/2)$ to all-to-all coupling. Note that the change of k from small to intermediate to large values corresponds to network variation from sparsely coupled to intermediately coupled to densely coupled network, respectively.

Through numerical experiments, we find that the number k has different influences on the coherence of the coupled systems under different coupling strengths, as shown in Fig. 9 ($g=10^{-2.5}$) and Fig. 10 ($g=10^{-2.0}$). The different values of k lead to different maxima of S [see Figs. 9(a) and 10(a)]. Moreover, the synchronization effect characterized by the ordering parameter R [Eq. (11)] also depends on k [see Figs. 9(b) and 10(b)], where for a fixed noise intensity, S in general decreases with increase of k (in other words, the larger k, the larger the synchronization region generally). More inter-

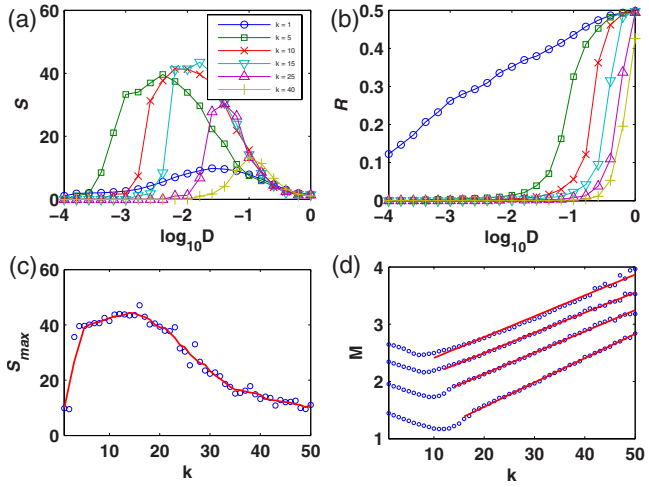

FIG. 10. (Color online) Influence of network topology degree k on dynamics of coupled systems with $g=10^{-2.0}$. (a) The coherence factor S vs noise intensity for several values of k. (b) The order parameter R vs noise intensity for the same values of k as in (a) [the colored curves correspond to those in (a)]. (c) The maximal value of S in observed noise range vs k. (d) Mean firing period M vs k for several values of noise intensity, from top to bottom: $D=10^{-1.0},10^{-0.8},10^{-0.6},10^{-0.4}$. The solid lines represent the linear fittings.

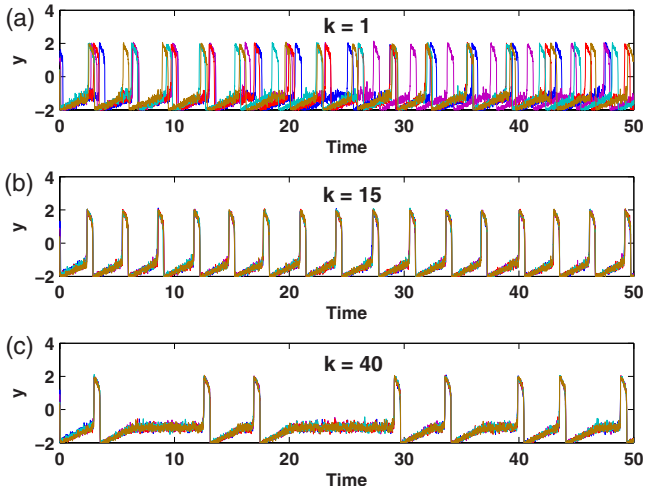

FIG. 11. (Color online) Time evolution of variable y in coupled SISR oscillators for $g=10^{-2.0}$ and several different network topology degrees, from bottom to top: $k=40$, 15, and 1. Five randomly selected oscillators from 100 are plotted in each panel.

estingly, for a small coupling strength (e.g., $g=10^{-2.5}$), the maximum of S as a function of k first goes down slowly with increase of k [see the inset of Fig. 9(c)], and then rises suddenly when k exceeds a certain threshold value (≈ 6). On the other hand, for a slightly larger coupling strength (e.g., $g=10^{-2.0}$), the maximum of S as a function of k has an optimal value [see Fig. 10(c)]. In other words, the coherence of the network with intermediate coupling is "better" than the those of sparsely and densely coupled networks. The results reported in Fig. 11 show that for both sparsely and densely coupled networks, the noise-excited oscillations appear to be rather irregular, whereas for intermediate coupling the noise-induced coherent oscillations are regular. This phenomenon is similar to the system-size resonance found in an ensemble of noise-driven bistable systems.

In addition, we also investigate the influence of k on the mean firing period [see Figs. 9(d) and 10(d)]. Surprisingly, the mean firing period decreases as k increases in the case of the sparsely coupled network [see the left part corresponding to small values of k in Figs. 9(d) and 10(d)]. As k goes through a threshold (which depends on noise strength) and further increases, the mean firing period begins to increase gradually. More interestingly, we find that the relationship between the mean firing period and the parameter k is linear when k passes the threshold for a fixed noise intensity [see the right part corresponding to large values of k in Figs. 9(d) and 10(d)].

VI. CONCLUSIONS AND DISCUSSION

In this paper, we have numerically investigated the interaction effect of coupling strength and noise intensities on coherence and synchronization in three cases: interacting SC and SISR oscillators, an array of coupled SISR oscillators, and density-coupled SISR oscillators. We have shown that, for interacting SC and SISR oscillators, the coherence depends not only on the coupling strength but also on noise intensities. More precisely, for weak coupling, the two oscillators are insensitive to each other, and the coupled system does not show any synchronization, whereas for strong coupling, a fixed stochastic oscillator can be entrained to the other adjustable stochastic oscillator [implying a phase locking can take place; see Figs. 4(d) and 6(d)] when the noise intensity of the latter is not beyond a threshold. Recently, Musizza *et al.* [39] have investigated interactions between cardiac, respiratory, and electroencephalogram δ oscillators in rats during anesthesia. They demonstrated that the three types of stochastic oscillators have different interactions under different phases in a noisy environment. Our results obtained here are in basic accordance with the phenomena they reported. In addition, for an array of coupled SISR oscillators, the effect of the array on coherence and synchronization is basically similar to the case of similarly coupled SC oscillators, but the array enhancement effect of the former is more remarkable than that of the latter under the same parameter conditions. For density-coupled SISR oscillators, we found an interesting phenomenon, i.e., an appropriate network topology degree induces optimal coherence. In other words, the system-size resonance found first in an ensemble of noise-driven bistable systems can take place in coupled SISR oscillators.

Since the coherence in a single SISR oscillator is better than that in a single SC oscillator [14], it is not surprising that many better properties for coherence resonance can occur in the case of interacting SISR oscillators than in the case of interacting SC oscillators. However, if a SISR oscillator interacts with a SC oscillator, whether or not coherence resonance or some kind of synchronization can be achieved has not been investigated before to our knowledge. Although we

have obtained some interesting results for this, some deeper questions deserve further investigation: Which of these two oscillators is dominant when synchronization is achieved? How does the parameter a affect coherence in interacting systems? Does the coherence resonance depend on a bifurcation point in the interacting systems?

Although we have shown that an appropriate network topology degree in density-coupled SISR oscillators can induce the best coherence resonance, a more interesting question is whether this property is generic. We will show that the answer is positive (the result will be presented elsewhere). Thus, we conclude that interacting stochastic oscillators have the following nice properties: array-enhanced coherence, system-size-induced coherence resonance, noise-induced phase synchronization, and network topology degree-induced coherence resonance or network topology degree-enhanced coherence. These properties altogether describe the rich dynamics of interacting stochastic oscillators.

Finally, we point out that, although two types of noise are observed in neurons, their competitive and cooperative effects and significance have not been fully elucidated. In our findings, the noise of the fast variable (whose levels are associated with the voltage noise levels observed in real neurons) may induce more coherent firing events. In addition, it should be noted that the fast and slow noise effects demonstrated here are quite general and can occur in other excitable systems with multiple time scales. In fact, experimental investigations of two coupled neurons from Retzius neurones of the leech [40] and from the stomatogastric ganglion of the California spiny lobster *Panulirus interruptus* [41] have showed various kinds of synchronization behaviors. The mechanism presented here based on the FHN model should be able to be used to interpret the experimental observations on the reliability of spiking timing of neurons and shed further light on understanding biological information processing [42–45]. We expect that these findings will stimulate further theoretical and experimental work which will significantly improve the performance of noise-induced oscillators.

ACKNOWLEDGMENTS

This work was supported by the Natural Science Key Foundation of People's Republic of China (Grant No. 60736028).

[1] A. T. Winfree, *The Geometry of Biological Time* (Springer, Berlin, 1980).
[2] A. S. Pikovsky, M. Rosenblum, and J. Kurths, *Synchronization—A Unified Approach to Nonlinear Science* (Cambridge University Press, Cambridge, U.K., 2001).
[3] J. Keener and J. Sneyd, *Mathematical Physiology* (Springer-Verlag, New York, 1998).
[4] L. Gammaitoni, P. Hänggi, P. Jung, and F. Marchesoni, Rev. Mod. Phys. **70**, 223 (1998).
[5] B. Lindner, J. García-Ojalvo, A. Neiman, and L. Schimansky-Geier, Phys. Rep. **392**, 321 (2004).
[6] Gang Hu, T. Ditzinger, C. Z. Ning, and H. Haken, Phys. Rev. Lett. **71**, 432 (1993).
[7] A. S. Pikovsky and J. Kurths, Phys. Rev. Lett. **78**, 775 (1997).
[8] O. V. Ushakov, H.-J. Wünsche, F. Henneberger, I. A. Khovanov, L. Schimansky-Geier, and M. A. Zaks, Phys. Rev. Lett. **95**, 123903 (2005).
[9] B. Lindner and L. Schimansky-Geier, Phys. Rev. E **61**, 6103 (2000).
[10] R. C. Hilborn and R. J. Erwin, Phys. Rev. E **72**, 031112 (2005).
[11] A. Zaikin, J. García-Ojalvo, R. Báscones, E. Ullner, and J. Kurths, Phys. Rev. Lett. **90**, 030601 (2003).
[12] F. Sagués, J. M. Sancho, and J. García-Ojalvo, Rev. Mod. Phys. **79**, 829 (2007).
[13] C. B. Muratov, E. V. Eijnden, and W. E, Physica D **210**, 227 (2005).
[14] R. E. Lee DeVille, E. Vanden-Eijnden, and C. B. Muratov, Phys. Rev. E **72**, 031105 (2005).
[15] C. B. Muratov, E. V. Eijnden, and W. E, Proc. Natl. Acad. Sci. U.S.A. **104**, 702 (2007).
[16] A. Neiman, L. Schimansky-Geier, A. Cornell-Bell, and F. Moss, Phys. Rev. Lett. **83**, 4896 (1999).
[17] P. Jung and G. Mayer-Kress, Phys. Rev. Lett. **74**, 2130 (1995).
[18] M. Perc, Phys. Rev. E **72**, 016207 (2005).
[19] S. Kádár, J. Wang, and K. Showalter, Nature (London) **391**, 770 (1998).
[20] J. F. Lindner, S. Chandramouli, A. R. Bulsara, M. Löcher, and W. L. Ditto, Phys. Rev. Lett. **81**, 5048 (1998).
[21] J. F. Lindner, B. K. Meadows, W. L. Ditto, M. E. Inchiosa, and A. R. Bulsara, Phys. Rev. Lett. **75**, 3 (1995).
[22] J. F. Lindner, B. K. Meadows, W. L. Ditto, M. E. Inchiosa, and A. R. Bulsara, Phys. Rev. E **53**, 2081 (1996).
[23] J. F. Lindner, M. Bennett, and K. Wiesenfeld, Phys. Rev. E **73**, 031107 (2006).
[24] B. Hu and C. S. Zhou, Phys. Rev. E **61**, R1001 (2000).
[25] C. S. Zhou, J. Kurths, and B. Hu, Phys. Rev. Lett. **87**, 098101 (2001).
[26] Y. Shinohara, T. Kanamaru, H. Suzuki, T. Horita, and K. Aihara, Phys. Rev. E **65**, 051906 (2002).
[27] O. Kwon, H.-H. Jo, and H.-T. Moon, Phys. Rev. E **72**, 066121 (2005).
[28] A. S. Pikovsky, A. Zaikin, and M. A. de la Casa, Phys. Rev. Lett. **88**, 050601 (2002).
[29] A. C. Scott, Rev. Mod. Phys. **47**, 487 (1975).
[30] X. Pei, L. Wilkens, and F. Moss, Phys. Rev. Lett. **77**, 4679 (1996).
[31] P. E. Kloeden and E. Platen, *Numerical Solution of Stochastic Differential Equations* (Springer-Verlag, Berlin, 1992).
[32] Z. F. Mainen and T. J. Sejnowski, Science **268**, 1503 (1995).
[33] J. A. White, J. T. Rubinstein, and A. R. Kay, Trends Neurosci. **23**, 131 (2000).
[34] S. K. Han, T. G. Yim, D. E. Postnov, and O. V. Sosnovtseva, Phys. Rev. Lett. **83**, 1771 (1999).
[35] D. E. Postnov, O. V. Sosnovtseva, S. K. Han, and T. G. Yim, Int. J. Bifurcation Chaos Appl. Sci. Eng. **10**, 2541 (2000).

[36] B. Hauschildt, N. B. Janson, A. Balanov, and E. Schöll, Phys. Rev. E **74**, 051906 (2006).
[37] G. V. Osipov, A. S. Pikovsky, M. G. Rosenblum, and J. Kurths, Phys. Rev. E **55**, 2353 (1997).
[38] C. J. Tessone, C. R. Mirasso, R. Toral, and J. D. Gunton, Phys. Rev. Lett. **97**, 194101 (2006).
[39] B. Musizza, A. Stefanovska, P. V. E. McClintock, M. Paluš, J. Petrovčič, S. Ribarič, and F. F. Bajrović, J. Physiol. **580**, 315 (2007).
[40] F. F. De-Miguel, M. Vargas-Caballero, and E. García-Pérez, J. Exp. Biol. **204**, 3241 (2001).
[41] R. D. Pinto, P. Varona, A. R. Volkovskii, A. Szücs, H. D. I. Abarbanel, and M. I. Rabinovich, Phys. Rev. E **62**, 2644 (2000).
[42] A. D. Dorval, Neuroscientist **12**, 442 (2006).
[43] Z. F. Mainen and T. J. Sejnowski, Science **268**, 1503 (1995).
[44] M. C. W. van Rossum, B. J. O'Brien, and R. G. Smith, J. Neurophysiol. **89**, 2406 (2003).
[45] V. M. Rodriguez-Molina, A. Aertsen, and D. H. Heck, PLoS ONE **2**, e319 (2007).